ATTENTION MICROFICHE USER,

The original document from which this microfiche was made was found to contain some imperfections that reduce full comprehension or some of the text despite the good technical quality of the microfiche itself. The failures may be:

- missing or illegible pages/figures;
- wrong pagination;
- poor overall printing quality, etc...

We normally refuse to microfiche such a document and request a replacement document (or page) from the national INIS Centre concerned. However, our experience shows that many months pass before such documents are replaced. Sometimes the Centre is not able to supply a better copy or, in some cases, the pages that were supposed to be missing correspond to a wrong pagination only. We feel that it is better to proceed with distributing the microfiche made of these documents than to withhold them till the imperfections are removed. If the removals are subsequently made then replacement microfiche can be issued. In line with this approach then, our specific practice for microfiching such documents is as follows:

1. A microfiche of an imperfect document will be marked with a special symbol (black circle) on the left of the title. This symbol will appear on all masters and copies of the document (1st fiche and trailer fiches) even if the imperfection is on one fiche of the report only.

2. If the incorrectnesses are not too general the reason will be specified on a sheet such as this, in the space below.

3. The microfiche will be considered as temporary, but sold at the normal price. Replacements, if they can be issued, will be available for purchase at the regular price.

4. A new document will be requested from the supplying Centre.

5. If the Centre can supply the necessary pages/document a new master fiche will be made to permit production of any replacement microfiche that may be required.

The original document from which this microfiche has been prepared has these imperfections:

|X| missing pages/figures numbered: p: 32 (Fig. 4).
|__| wrong pagination
|__| poor overall printing quality
|__| combinations of the above
|__| other

INIS Clearinghouse
I.A.E.A.
P.O. Box 100
A-1400, VIENNA
AUSTRIA

Not reviewed version

Invited paper for 8 International Symposium on Thermodynamics of Nuclear Materials, STNM 92, Snowbird, Utah, August 16-21, 1992, Proc J Nucl Mater

THERMAL AND PHYSICOCHEMICAL PROPERTIES IMPORTANT FOR THE LONG TERM BEHAVIOR OF NUCLEAR WASTE GLASSES

Hj. Matzke + and E. Vernaz*

+ Commission of the European Communities, Joint Research Centre, Institute for Transuranium Elements, Postfach 2340, W 7500 Karlsruhe, Federal Republic of Germany
* Centre d'Etudes Nucléaires de la Vallée du Rhône, SCD, BP 171, F-30207 Bagnols-sur-Cèze, France

ABSTRACT

High level nuclear waste from reprocessing of spent nuclear fuel has to be solidified in a stable matrix for safe long-time storage. Vitrification in borosilicate glasses is the technique accepted worldwide as the best combination of engineering constraints from fabrication and physicochemical properties of the matrix. A number of different glasses was developed in different national programs. The criteria and the reasons for selecting the final compositions are briefly described.

Emphasis is placed on the French product R7T7 and on thermal and physicochemical properties though glasses developed in other national projects (e.g. the German product GP 98/12 etc.) are also treated.

The basic physical and mechanical properties and the chemical durability of the glass in contact with water are described. The basic mechanisms of aqueous corrosion are discussed and the evolving modelling of the leaching process is dealt with, as well as effects of container material, backfill, etc. The thermal behavior has also been studied and extensive data exist on diffusion of glass constituents (Na) and of interesting elements of the waste such as the alkalis Rb and Cs or the actinides U and Pu, as well as on crystallization processes in the glass during storage at elevated temperatures. Emphasis is placed on the radiation stability of the glasses, based on extensive studies using short-lived actinides (e.g. Cm-244) or ion-implantation to produce the damage expected during long storage at an accelerated rate. The radiation stability is shown to be very good, if realistic damage conditions are used.

The knowledge accumulated in the past years is used to evaluate and predict the long-term evolution of the glass under storage conditions.

1. Introduction

During fabrication, use and consumption of any goods, waste products are formed which have to be disposed of in a safe way. This is, of course, also true for the peaceful use of nuclear energy from electricity producing power stations. Some of the radioactive nuclides formed in a nuclear reactor, either by fission or by transmutation following neutron capture, have long half-lives. Dispersible high-level nuclear waste (mostly in liquid form from reprocessing, but also sludges and ashes) have to be solidified in a stable matrix and disposed of in a suitable repository, e.g. a deep dry geological formation in order to minimize the possibility of radionuclides reaching the biosphere. A large number of matrices has been proposed and studied. The currently favored technology is vitrification of the waste, i.e. its incorporation into special tailor-made borosilicate glasses. Other matrices that were investigated are phosphate glasses, glass ceramics, and tailor-made ceramics such as SYNROC (a synthetic rock), supercalcine and others. These matrices were recently described in a book edited by Lutze and Ewing [1].

The radioactive high level waste (HLW) contains typically some 40 different elements: fission products, ranging from Ga to the rare earth Dy, corrosion products from the cladding of the fuel elements (usually the Zr-alloy Zircaloy), steel components (Fe, Ni, Cr) from plant equipment, Na from alkaline rinse, P from TBP decomposition, some actinides (some Pu and Cm, but mainly U, Np and Am) and some insoluble particles such as Zr fines from the cladding of the fuel elements or platinoids. Borosilicate glasses have the capability of incorporating most of these elements. They were chosen as the best compromise between fabrication engineering constraints and the physicochemical and thermal properties of the final product, i.e. between requirements of technical feasibility and highest possible degree of containment. For large scale fabrication, the processing temperature (viscosity of the molten glass, corrosion rates between molten glass and furnace and/or container materials, minimization of evaporative losses during fabrication, of e.g. Rb and Cs) is of importance, and for safe long time storage, the material must be capable of incorporating virtually all of the about 30 chemical elements occurring in high level waste, it must show a high resistance against aqueous corrosion and a low susceptibility for radiation damage effects as well as a high resistance against recrystallization. Very much research efforts have been devoted to develop glasses suitable for different waste streams. Obviously, optimizing one of the above properties alone is not advisable; rather the choice of the glass is made in a way that all necessary properties are optimized to a satisfactory extent.

Vitrification plants for fully active borosilicate glasses exist at various places, e.g. in France, Belgium, the UK and India. The largest plants are located at the reprocessing factory at La Hague in northern France. The French reference glass for LWR fission product solutions, SON 681817, generally referred to as "R7T7" glass [2], is mainly described in the following since it is the glass most widely used. Some results will also be given for the German glass GP 98/12 [3] though it will not be technologically used in the near future since reprocessing of German fuel will not be done in Germany.

2. The nuclear fuel cycle, high level waste (HLW) and conditions for safe storage of solidified HLW in deep geological formations

To better understand the physics and chemistry of solidified high level waste (HLW) and its storage conditions, a brief recollection of the fuel cycle, of composition and radiation of HLW and of storage conditions will be given.

Electricity-producing nuclear power stations utilize the heat produced by fissioning U or Pu atoms contained in the fuel, normally UO_2 in a Zircaloy sheath. Most neutrons are used for fission but some are captured by U and Pu-atoms. Due to subsequent β-decays, higher actinides can be formed (Am, Cm etc., and also Np). After a few years of operation, corresponding typically to a burnup of 3 to 5 % of the heavy metals (U and Pu), depletion in fissile atoms, capture of neutrons by fission products as well as radiation effects in the fuel and corrosion of the clad cause continued operation of the fuel to be not economic. The fuel may then be either stored or disposed of as spent fuel, or it is reprocessed to recover the unused vast majority of U (and Pu formed during operation). To this end, the fuel is dissolved in nitric acid and the re-usable U and Pu are chemically separated. The resulting unusable liquid and some insoluble sludges contain only a very small fraction (< 1 %) of the U and Pu, but all the fission products, the other actinides and some corrosion products (Zr, Fe, Ni, Cr etc.). The exact composition of this HLW depends on burnup, reactor strategy, neutron spectrum, duration of reactor shutdowns, storage time before reprocessing and age of the HLW. The reason is that radioactive decay and transmutation processes by neutron capture constantly change the relative concentration of individual nuclides and elements in the fuel or in the waste. The glass composition must therefore be adopted to each type of fission product solution.

As an example, a typical composition of HLW solutions obtained at the French reprocessing station La Hague, for a 33000 MWd/t PWR fuel, is given as an indication. Per ton of reprocessed U are obtained

- about 300 l of liquid waste (2 N acid solution)
- about 135 l HLW containing insoluble residues from liquid clarification by centrifugation
- this HLW contains about 38 kg HNO_3, 29 kg of fission products (mainly Ba, Ce, Cs, Eu, Gd, La, Nd, Mo, Pd, Pr, Rb, Rh, Ru, Sm, Tc, Y and Zr), 6 kg Fe, 2.3 kg of Ni, Cr, P etc., 2.2 kg of the clad (mainly Zr), about 0.75 kg U, 0.05 kg Pu, 0.32 kg Am, 0.43 kg Np and 0.03 kg of Cm
- the corresponding activity, 4 years after the end of the irradiation, is about 600000 Ci (1 Ci = 3.7×10^{10} Bq) of β, γ radiation and 2800 Ci of α-radiation.

Borosilicate glasses contain conventionally network modifiers (e.g. Li,Na) and network formers (e.g. Al, or Ti for GP 98/12). With different concentrations of these and other additives, tailor-made glass properties can be achieved. As examples, one can mention Li which can decrease the formation temperature and the electrical resistivity; Al, as network former - occurring in AlO_4 tetrahedra - increases glass stability and chemical durability, but increases also the melting temperature; Ti, another network former, reduces Cs-volatility (in GP 98/12), but may act as nucleation agent for crystallization; CaO, MgO and ZnO affect the viscosity; ZnO reduces also the melting temperature, etc. To produce a tailor-made glass, a large number of glasses with slightly different compositions are fabricated and tested and the best product is finally selected.

The R7T7 glass was developed based on the results of several years of such research, to optimize its properties with the aim to vitrify the HLW generated by reprocessing PWR fuel. Its composition is given in Table 1 and some relevant properties are summarized in Table 2; the German product GP 98/12 is also included in these tables.

Due to the radioactive decay of the fission products, the waste glass experiences increased temperatures which decrease with storage time, essentially following the decay of Sr-90 and Cs-137 such that the repository temperature is reached after about 500 years. Waste contents are chosen in such a way that the central temperature of the glass blocks does not exceed some specified value during interim storage, e.g. 450 °C for the French glass R7T7. The maximum surface temperature in the final repository is not yet specified but will be much lower, depending on disposal concept and interim storage duration. The crack pattern in the glass blocks is a further important parameter [4] for the radial temperature profile in the glass blocks. Because of the increased temperature, the kinetics of recrystallization and of diffusion of interesting elements has been

studied not only with respect to fabrication but also with respect to storage. The evidence obtained is described below.

The waste glass also experiences radiation damage. Due to the high initial activity of β-, γ-emitting fission products, most of the (cumulative) decay events and most of the (initial) ionizing dose are due to β-decays. The actual total number N of defects produced in a given time span depends on the type (age etc.) and concentration of HLW in the glass, whereas the relative ratios are less affected. For instance, assuming again the 33000 MWd/t burnup, but 5 years cooling before reprocessing and a high loading of 25 wt.% HLW [e.g. 5-7], about $2x10^{26}$ β-decays/m^3 occur typically within the glass in the first 1000 years, whereas even after 10^5 years, only about $3x10^{25}$ α-decays have occurred. The corresponding ioniziation doses are very similar: about $1x10^{12}$ rad for both β-, γ-emission and for α-decays Most atomic displacements, however, are due to the α-decays. The reason is that electrons (β-particles) produce very few displacements ($N \leq 1$). In contrast, α-particles produce about 200 defects, and the heavy recoil atoms of the α-decay, (e.g. U in the decay of Pu, with a recoil energy of ~ 100 keV) lead to $N \sim 1200$. Consequently, whereas α-decay events produce near to 10^{29} displacements/m^3 for the above waste in 10^5 years, β-, γ-decays produce only a small fraction of this number, i.e. ~ $3x10^{25}$ cumulative displacements/m^3. The contribution of spontaneous fission (e.g. of Cm) is very small. Because of the dominating effect of the ~ 100 keV heavy recoil atoms of the α-decay in producing atomic displacements in the glass, damage effects have widely been studied using both radioactive decay of short-lived actinides and simulation techniques employing energetic beams of heavy ions in the energy range of 10^2 keV to produce the damage [e.g. 6, 7].

For the unlikely event of ground water having access to the repository, the kinetics of aqueous corrosion have to be investigated and the possible effects of damage have to be elucidated. Extensive results exist for the R7T7 glass [e.g. 8, 9] and are summarized below. A large variety of experimental surface analysis techniques [e.g. 10, 11] in combination with careful chemical analyses was used to obtain detailed results on kinetics of leaching and composition of the leached layers. Of course, other borosilicate glasses besides R7T7 and GP 98/12 have also been investigated extensively. Examples are the glass of the Pamela vitrification plant in Mol, Belgium, i.e. the glass SM 58 LW 11, or the US product MCC - or PNL-76-68 etc. (see refs [1, 12]).

Following on-ground controlled intermediate storage of the glass blocks, these will be disposed of in a suitable dry repository in a deep geological formation.

Candidates are granite formations, rock salt domes and clay formations. In these repositories, the access of water to the glass is very unlikely. In addition, the glass is protected by a metal container surrounded by a suitably chosen material (backfill) to fill the hole originating from drilling the shafts and cavities for the glass blocks. To realistically measure the leaching behavior of the glass, allowance must be made for the type of ground water, or salt brine, to be expected in the anticipated repository, and possible effects on solution chemistry of the presence of container material and backfill should be considered.

3. Thermal and physicochemical properties

The thermal and physicochemical properties of importance for fabrication and long term storage of waste glasses are determined on nonradioactive glass specimens containing inactive fission products (or "simulated waste"); these glasses are produced either on a laboratory scale or fabricated in a full-scale continuous vitrification prototype facility. To study the effect of radiation damage, parallel measurements are done on specimens produced in the laboratory or in the hot cells which contain either short-lived actinides (e.g. Cm-242, Cm-244 or Pu-238) or fully active HLW.

Thermodynamic measurements (e.g. Knudsen cell vapor pressure measurements reporting $NaBO_2$ etc. in the gas phase [e.g. 13]) have been performed over the glass melt, and the factors determining loss of radioactive fission products (e.g. Cs-137 but also Ru, Tc, Se etc.) during glass melting have also been studied, but most work was devoted to characterize the solid glasses and to determine their properties. We will therefore restrict ourselves in the following on properties and performance of solid glasses.

3.1. Composition and Homogeneity

The composition of the two glasses treated here is given in Table 1. The basic working philosophy for developing tailor-made glasses and some remarks on the reasons for adding oxides like CaO and Al_2O_3 to the borosilicate matrix have been given in Section 2. The final glass is a black product which is largely homogeneous at a μm scale. Some precipitates and second phases exist as heterogeneities. These are inclusions of some 10 - 20 μm size of metals (platinoids, Mo) of limited solubility, some RuO_2 inclusions, some chromites containing Fe, Ni and Cr if a metallic (Inconel) melting pot is used, some gas-filled bubbles and the "yellow phase", i.e. alkali or alkaline earth molybdates These phases constitute

less than 1 vol.% of the glass, proving the very good homogeneity of the final product.

3.2 Physical and mechanical properties

Table 2 summarizes the main physical and mechanical properties for the simulated HLW glasses R7T7 and GP 98/12. These properties are not very different from those of conventional industrial glasses. Note, however, that the mechanical properties are superior to those of window glass or pyrex, to mention two conventional glasses.

Of particular interest for long term storage are hardness, H, and fracture toughness, K_{Ic}. Both will be shown to be affected by radiation damage in a beneficial way for storage (see Section 5). The fracture toughness, i.e. the critical stress intensity at which extension of a preexisting crack or flaw occurs, is (ideally) a material constant independent of specimen geometry describing the resistance of a material against fracture. Different test methods were used to measure K_{Ic} on French waste glasses by one of the present authors [14]: biaxial flexure, double torsion and the short rod test. The use of indentation techniques with both sharp (Vickers diamond) and blunt (Hertzian sphere) indentors was extensively applied by the other author as summarized in two proceedings of workshops specialized on indentation techniques [15, 16]. Indentation techniques are particularly useful for highly radioactive specimens such as Cm-doped glasses or for ion-implanted glasses of which specimens of limited size only are available since statistics can be obtained on a small size specimen [e.g. 17-19]. The short rod fractometry test method was modified to measure several K_{Ic}-values on the same glass specimen [20]. The agreement of all these measurements was very satisfactory. The resulting values are included in Table 2, and the dependence of K_{Ic} on radiation damage (see Section 5) and temperature are known [21, 22].

3.3 Thermal stability and recrystallization

As mentioned above, the nuclear waste glasses produce heat due to the radioactive decay of the HLW. The thermal power of the R7T7 glass is about 7 W/kg at the time of fabrication, dropping to about 1 W/kg after 50 years and to ~ 0.05 W/kg after 300 years. The question of possible recrystallization during this period is of importance since partial crystallization could negatively affect the integrity of the glass blocks, it could introduce cracks or porosity into the originally homogeneous glass, and it could change the composition of the glass and

thus the chemical and physical properties, e.g. it could increase leach rates. Much work was therefore devoted to adjust the composition of the finally selected glass to minimize its tendency towards crystallization. The incipient temperature below which no growth of crystals is observed, is used to define the maximum storage temperature with a good margin of safety. This incipient temperature is 600 - 620 °C for R7T7. The maximum crystallization temperature is typically 780 °C for R7T7. Annealing tests at this temperature provide a means to determine the maximum fraction of crystal volume liable to form during long-term storage. This fraction increases with the amount of second phases of insoluble platinoids and chromites but never exceeds a few volume percent for R7T7. It was shown to have no significant effect on the properties of the glass [e.g. 2].

3.4 Diffusion in Waste Glasses

Knowledge on diffusion processes in waste glasses is important for a number of reasons. Diffusion phenomena affect second phase formation and crystallization, they are important for formation of surface gradients, e.g. during leaching and the interdiffusion of Na and hydrogen or hydronium ions is a basic step in forming leached layers. Data on the diffusion of the alkali elements are also needed to understand and predict their migration in the temperature gradients existing in waste glass cylinders, and to estimate the importance of the "mixed alkali effect", i.e. the very pronounced dependence of alkali ion mobilities on the relative concentrations of the different alkalis [e.g. 23].

Diffusion processes have therefore been studied in detail for a number of elements including the alkali elements Na, Rb, Cs, the fission products Te and Pd which are known to tend to precipitate in the glasses, and the actinides U and Pu [23-28]. The glass GP 98/12 containing simulated HLW (see Table 1) or the base glass without added simulated HLW, called VG 98/12 were used for the diffusion of Na, Rb, Cs, Te and Pd whereas a precursor of GP 98/12 was used for actinide diffusion studies. Both tracer techniques (Na,Rb,U,Pu) and Rutherford backscattering of 2 MeV He-ions (for Rb, Cs, Te and Pd) were applied to measure diffusion profiles following annealing. Fig. 1 summarizes the results in an Arrhenius diagram.

Na-diffusion is very fast and can be described by the relation (D in $cm^2 s^{-1}$, ΔH in eV)

$$D^{Na} = 0.015 \exp(-1.08\ kT)$$

It is well known that the alkali elements migrate in glasses, including waste glasses, by radiation-enhanced diffusion under irradiation by external beams of electrons, protons or heavy ions even at room temperature [29]. In these cases, the migration of Na becomes biased in the electric field gradient due to the charging effect caused by the external beams of ions or electrons. For example, under EDAX or Auger analysis (i.e. electron irradiation) at room temperature of the present waste glasses, one observes a fast disappearance of Na at the irradiated surface. Similarily, waste glasses (and other simpler borosilicate glasses) which are ion-implanted at room temperature with heavy ions, show a pronounced surface enrichment in Na. However, these phenomena are only seen after a certain incubation time. These observations were modelled by Mazzoldi, Miotello and Toigo [29, 30] applying the Onsager formalism of irreversible thermodynamics and allowing for the electric fields set up by the external beams. These authors could show that D^{Na} is increased by factors of 10^5 to 10^6 by the above irrradiation at room temperature; the activation enthalpy decreases from the above 1.1 eV (without irradiation) to a few hundredth of an eV. To explain the incubation time, the authors proposed breakage of Na-O bonds to create an oxygen defect. A first fast step of defect recombination (within msec) leads to a more stable structurally relaxed unit with a lifetime of minutes. Though the Na-ions can easily migrate in the relaxed structure, a migration on a macroscopic scale is only possible if these units form disordered channels in a relaxed "lattice". The concentration necessary for percolation (~ 1/3 to 1/4) is obtained in the incubation time. This explains also the observed absence of enhanced Na-diffusion for pulsed irradiations.

These conditions are, however, different from those of damage formation in real waste glasses where no net charge is formed and where dose rates are smaller. Recent experiments on Na-22 tracer diffusion under α-irradiation using GP 98/12 doped with Pu-239 or Cm-244 showed no significant radiation enhancement [28]. The reason is that overlap of damaged zones occurs only about twice per week, even for the short-lived Cm-244, a time too long to build up the percolation-allowing relaxed "lattice" described above. The pronounced enhancement of Na-diffusion observed under electron or ion-beam irradiation is thus not occurring under α-irradiation and realistic storage conditions.

Rb- and Cs-diffusion: The fission product alkali elements, Rb and, in particular, Cs (important for storage because of the 30 years half-life and the intense γ-radiation of Cs-137) could, in principle, also show mobilities affected by the mixed alkali effect. For Rb, tracer diffusion with radioactive Rb-83 and Rb-84 was measured [23]. Rutherford backscattering analysis was used to determine

diffusion profiles of (inactive) Rb and Cs following annealing of ion-implanted VG 98/12 and GP 98/12. Rb and Cs diffuse much more slowly than Na (see Fig. 1) and there was no obvious effect of the added (simulated) waste. The resulting Arrhenius plots were curved. Because of the small diffusion coefficients, the experimental temperature range was extended to above the glass transformation temperature T_t (= 543 °C, see Table 2) and even slightly above the softening point, T_s (= 607 °C). As expected, annealing of the glass at temperatures higher by more than some 30 °C than T_s caused deformation of the plastic glass. No effects of recrystallization were seen, confirming the good performance of the final glass product, as described in Section 3.3, and in contrast to the behavior of earlier (precursor) glass products (see U-diffusion, below).

For Rb, a straight line could be fitted through the experimental data (18 specimens, not shown separately in Fig. 1 which shows scatter bands) for $T < T_t$ described by

$D^{Rb} = 0.5 \exp(-1.9/kT)$ for ion implanted glasses

$D^{Rb} = 0.0015 \exp(-1.5/kT)$ for undamaged glasses (gas phase or sandwich).

Below 500 °C, the data for radioactive tracers (labelling via the gas phase or in a sandwhich arrangement, hence without damage) were higher than those obtained with ion-implanted specimens. This indicates trapping of Rb at damage centres, as it is known to occur with hydrogen in ion implanted glasses and fused silica [e.g. 31]. Radiation damage, while enhancing diffusion during its formation, e.g. by bond breakage and atomic mixing in the collision cascades, creates thus also trapping sites for Rb ions moving by thermally activated diffusion. Annealing at temperatures at or above ~ 500 °C is necessary to release Rb from these traps. Because of the complex structure of the multicomponent waste glass, the nature of the trapping defects cannot be specified yet. Similar trapping and release phenomena were also observed for Kr- and Xe-implantation into GP 98/12 [26] and R7T7 [32] for which the same size effect was seen as shown in Fig. 1 for Rb and Cs. For the latter, the curvature in the Arrhenius diagram prevented any determination of a single set of D_0- and ΔH-values. It is premature to suggest mechanisms for these diffusion processes. However, the results are compatible with suggested compensation laws as applied earlier by Kahl [33].

An evaluation of all results for Rb and Cs shows that the diffusion of the heavy alkalis is very slow. Even if allowance is made for the mixed alkali effect [23], the thermal diffusion of Rb and Cs in the temperature gradients existing in full scale, fully active waste glass cylinders can safely be considered to be very slow, too.

Diffusion of Te and Pd: Rutherford backscattering analysis was recently used in an attempt to measure the diffusion of Te and Pd, two fission products known to form precipitates in waste glasses [27]. As shown in Fig. 1, Te diffusion was very slow indeed and showed a very high *apparent* activation enthalpy ΔH of 5.5 eV atom. The cause for this high value is probably the fact that temperatures above T_t had to be used to obtain measurable penetration profiles. Below 500 °C, diffusion was negligible. No measurable diffusion was observed with Pd. The reason is its limited solubility - actually determined in the same study to be ~ 0.05 at%. Accordingly, SEM analysis following the diffusion anneals showed indeed small precipitates at the surface. These data indicate that Te separation to the surface, or precipitation (e.g. as Pd-telluride) would only occur during glass production and that Pd diffusion would only proceed until the Pd precipitates are formed.

Actinide diffusion: the tracer diffusion of U-233 and of Pu-238 was measured in a precursor version of GP 98/12 [24, 32]. As shown in Fig. 1, diffusion of U is very slow. Similar results were obtained for Pu. Since the non-destructive technique of α-spectroscopy [e.g. 34] was applied, the same diffusion couple could be used for several anneals at the same temperature, thus enabling to follow the time dependence of diffusion. In this way, changes in the specimen morphology leading to changed diffusion rates can easily be observed. Fig. 2 shows typical data for a precursor glass of GP 98/12 not yet optimized against recrystallization. Also, since the same specimen was used to obtain all of the data of Fig. 2, nucleation for recrystallization was facilitated by the long preanneals at lower temperatures. The diffusion coefficients in the glass were, as expected, independent of time with very low values of $D^U = 8 \times 10^{-18}$ cm^{2}s^{-1} at 500 °C and $D^U = 4 \times 10^{-17}$ cm^{2}s^{-1} at 540 °C. Recrystallization kinetics could be followed by observing the time dependence of U-diffusion as verified by parallel optical microscopy and X-ray analysis. In the resulting glass ceramic, i.e. at $T \geq 620$ °C, D^U was again independent of time, but lower than D^U in the glass. As an example, the diffusion coefficients in the glass at 540 °C are practically identical to those in the glass-ceramic at 620 °C. Note, that this type of behavior was only observed with not optimized precursor glasses.

No significant effect of α-decay was seen in glasses with 4.7 wt.% added americium. Cm-doped glasses with a total damage level of 1.1×10^{25} α-decays/m^3 (corresponding to a storage time of about 10^4 years [e.g. 35]) showed an accelerated diffusion for a short time only when annealed at temperatures at which the stored energy is released (380 to 500 °C). The total amount of tracer penetration was

proportional to the amount of stored energy and was never larger than ~ 3 µm. In conclusion, U and Pu diffusion are negligible at the temperatures existing in glass blocks. As with Na-diffusion, no significant radiation-enhancement is observed.

4. Chemical durability, leaching behavior

For safety assessments for the case of water having access to the repository, the kinetics of leaching under different possible conditions (type and composition of leaching solution, pH, temperature, radiation etc.) must be known and have been studied in detail.

The inherent resistance of a glass towards aqueous corrosion can be characterized by its initial dissolution rate in pure water. Two types of experimental conditions can be applied to measure this basic leach rate:

a) **dynamic experiments** in which the glass is in contact with continuously renewed water, e.g. in a so-called Soxhlet experiment, in which the water is continuously re-distilled and the experimental temperature is therefore 100 °C.

b) **static experiments** in which the initial shape in a plot of leach rate vs. time for the main elements in the glass as well as the total weight loss are measured. The amount of water, expressed as ratio of glass surface S, to water volume V, hence S/V, and temperature T are the main parameters. The temperature is ≤ 100 °C, if atmospheric pressure is used; for temperatures ≥ 100 °C autoclaves are used. For R7T7, this initial rate, r_0, is typically 1.7 $gm^{-2}d^{-1}$ (or 0.17 mg $cm^{-2}d$) at 100 °C (see Fig. 3). For these measurements, the surface of the reacting glass is assumed to be the calculated geometric surface area of monolithic samples. This approximation is particularly good after a few days of glass leaching (at 100 °C) since glass dissolution produces a chemical polishing which strongly reduces the initial roughness of the polished sample. The temperature dependence of r_0 is described by an Arrhenius law with an activation enthalpy of 60 $kJmol^{-1}$ [36]: r_0 depends also on the pH of the leaching solution, increasing for R7T7 by about a factor of 10 if the pH increases from 7 to 10 [37].

Dynamic experiments with a high flow rate, as Soxhlet, are absolutely not relevant for geological storage conditions; they are only useful to determine the initial rate of glass dissolution. Static experiments may be not totally relevant either since a low flow rate of underground water has to be considered in the risk assessment. However, in most geological formations this flow rate is so low that

static experiments can often be regarded as the best approximation for laboratory scale experiments.

The normalized mass loss NL can be obtained either from the mass loss (Δm in g) of the specimen with surface S(m^2)

$$NL_m = \Delta m/S$$

or from the element analysis in the leaching solution

$$NL_i = (C_i x V_i) / x_i S$$

where NL_i = normalized mass loss (gm^{-2}) for element i, C_i its concentration (gl^{-1}) in solution, V_i the solution volume and x_i the concentration of element i in the glass.

As with the mechanical properties (see Section 3.2), the leach resistance of waste glasses is better than that of soda-lime "window glasses", though it is slightly inferior to that of pyrex glass. As an example, the normalized mass losses (total, Si and Na, in this order, in gm^{-2}) are, for a static test for 1 week at 90 °C with S/V = 50 m^{-1}, for the soda-lime glass 5.6; 5.6; 12.0; for R7T7 0.9; 1.8; 1.8; and for pyrex glass 0.4; 0.1; 0.9.

If extrapolated to room temperature with the above activation enthalpy of 60 kJ/mol, the mass losses decrease to the order of a $\mu g/cm^2 d$, or less. To get quantitative information for such small changes, corresponding to leached layers of nm-thickness, radiotracer methods are useful. An example is shown in Fig. 4 where R7T7 glasses were implanted with a trace amount of radioactive Kr-85, and the loss of Kr-85 with progressing leaching in H_2O at 20 °C with S/V = 20 m^{-1} was measured as a function of time. The median range of Kr at the energy used (40 keV) is about 25 nm, i.e. 50 % of the implanted Kr are located within the first 25 nm. For the trace implant ($\sim 10^{12}$ ions/cm^2), the fractional Kr-loss corresponds to a leach rate of ~ 10 nm/week. The fractional Kr-loss is not completely linear with time since the Kr-range curve is peaked at the median range. The fact that leaching is significantly increased for high Kr-doses (high damage levels) is discussed in Section 5. It does *not* imply that high damage levels necessarily increase the leaching of waste glasses to a large extent (see below).

Though the above initial dissolution rates are an important indication of the chemical stability of the glass, they are not the main quantity affecting the long-term stability of the glass and its long-term alteration kinetics. To understand and predict these properties, the basic mechanisms of aqueous corrosion have to be known. These are

- **hydration and interdiffusion of $H^+ \rightleftharpoons Na$.** Following an initial hydration process, a reaction zone is formed in which this interdiffusion process occurs. This is the phenomenon dominating in acid media, and resulting in selective dissolution of the elements of the glass
- **dissolution of the silica network.** Most frequently, the leaching of alkali metals from the glass causes the pH of the solution to increase to alkaline levels. Under such conditions, the dissolution rate of the silica network is larger than that of interdiffusion. Consequently, a hydrated layer penetrates into the pristine glass at a rate r. For most silicate minerals, this rate r is controlled by the activity of the silicic acid in the solution, with a first-order relation. This relation is given by [38] $r = r_0 [1-(a_{Si}/a^*_{Si})]$ where r_0 is the initial dissolution rate, and a_{Si} and a^*_{Si} are the H_4SiO_4 activities in solution and at saturation, respectively (see also Fig. 5). With the complex waste glasses, there is an additional important phenomenon influencing aqueous corrosion, i.e.
- **formation of chemically altered surface layers.** Though all glass components become hydrated during the silicate network dissolution, many of the waste components form hydroxides, hydrosilicates or hydrated oxides which have a low solubility in alkaline solutions. Most of these elements remain at the glass surface and form an amorphous gel layer. In other words, though glass dissolution remains nonselective, i.e. all glass components are hydrated simultaneously, it becomes incongruent, since not all elements go into solution.

This gel layer affects the leaching kinetics in two ways: 1) it acts as a diffusion barrier which impedes the transport of silicic acid from the pristine glass surface where it is formed. Consequently, an activity gradient of H_4SiO_4 is established in the interstitial water of the gel. The above equation is thus modified: $r = r_0[1-(a_{Si}^{interl}/a^*_{Si})]$. 2) The gel traps also a fraction f of the hydrated silica by chemisorption. f is essentially a linear function of the silicon concentration in solution [39]: $f(\%) = \alpha(Si) + \beta$. At 90 °C, as saturation conditions are approached, about 75 % of the hydrated silicon remains trapped in the gel layer.

4.1 Modelling of the leaching behavior of the R7T7 glass

Based on the above observations, a mechanistic model for the aqueous corrosion was developed at Marcoule [8, 9]. The model called LIXIVER describes

the chronological evolution of the dissolution rates, the silicon concentration at the reaction interface, and the concentrations of glass matrix components in solution up to 300 °C for different glass and solution compositions under static or dynamic leaching conditions. The model combines the equations governing surface reaction and diffusion mechanisms, with an empirical law of partial silicon retention in the leached altered layer. It thus accounts for the following features:

i) the rate of glass dissolution is described by a first order relation

$$r = r_0 (1 - C_{Si}^{interf} / C^*_{Si}).$$

Here, concentrations are used rather than activities, considering the low ionic strength (see Fig. 5 where the indices "Si" have been omitted and "int" is used for "interf").

ii) C_{Si}^{interf}, i.e. the concentration of Si at the interface gel/glass, is iteratively calculated with a constant (apparent) diffusion coefficient D* for H_4SiO_4 and a linear concentration gradient in the gel, as shown in Fig. 5, where P indicates the concentration in the solution and C_{slb} the "solubilisable" Si-concentration, i.e. the difference between the Si-concentration C_0 in the pristine glass and the Si-concentration trapped in the gel, i.e. the other quantities used to calculate C_{int}.

iii) The value of C_{Si}* is recalculated at each step in the dissolution experiment allowing for the measured pH-value and for dissociation of silicic acid. Typical relations used are

$$SiO_2 + 2H_2O \overset{K_s}{\rightleftharpoons} H_4SiO_4 \qquad \log K_s = -3.0 \quad (90\,°C)$$

$$H_4SiO_4 \overset{K_1}{\rightleftharpoons} H^+ + H_3SiO_4^- \qquad \log K_1 = -9.17 \quad (90\,°C)$$

$$H_3SiO_4^- \overset{K_2}{\rightleftharpoons} H^+ + H_2SiO_4^{--} \qquad \log K_2 = -10.70 \quad (90\,°C)$$

iv) The fraction f of hydrated Si in solution is described by a linear relation, e.g. $f = 0.10 + 0.115\ [Si]$ where the concentration [Si] is given in mgl^{-1}.

For these conditions, good fits of the experimental data are obtained, as shown in Fig. 6. We can conclude that a first order law may be employed to describe the aqueous corrosion of the waste glass R7T7 in pure water, provided allowance is made for the above phenomena of importance for the formation of the leached layer.

The LIXIVER model does not intend to describe the solution behavior for very long times, but rather to investigate the effects of leaching parameters on the dissolution kinetics within the normal time scale (a few months to a year) of

laboratory experiments. The conditions at very long leaching times are described in Section 6.

4.2 Influence of repository, container and backfill materials

The nature of the repository materials (granite, salt or clay) and of the nearfield engineering barrier (e.g. steel, Hastelloy, Ti, etc. for the container, sand etc. for the backfill) are extremely important for the leaching process. Two examples are given here to illustrate this point: i) Most of the clays (smectite, illite, Boom clay) consume part of the silicon released into the medium during glass corrosion. As a result, the initial leach rate is determining leaching over a longer period of time keeping the leach rate at values near those observed in tests with constant leachate renewal [e.g. 19], ii) similarly, in the presence of a (corroding) steel container, a comparable effect is observed [e.g. 6] due to Si being absorbed (or reacting with) precipitating iron hydroxides. Because of the multiplicity of parameters operating in geological repositories, integral experiments simulating some or all of the disposal conditions are necessary to validate the basic models under realistic conditions. Such integrated test mockups referred to as "TAV" experiments (Test d'Altérations des Verres - glass alteration test) are extensively used in France to simulate possible storage scenarios [e.g. 19]. Space limitations do not allow to give more details in this article, but the topic will be briefly taken up again in Section 6.

5. Radiation stability of the waste glasses

As described in Section 2, the glasses experience large levels of radiation during long-term storage. Most atomic displacements are formed by the recoil atoms of the α-decay, whereas roughly equal amounts ($\sim 10^{12}$ rad) of ionization damage are produced by β-γ and α-decay (see Section 2). Damage effects have therefore extensively been studied in the past 15 years [e.g. 5-7, 17-19, 40-45], a workshop [7] was devoted to this question and an international standard [35] was worked out to relate damage in laboratory specimens containing short-lived actinides to the time scale of real storage. Though only small amounts of α-emitters are present in the waste glasses (~ 0.3 wt.%, corresponding to only about 0.1 at%, excluding U), most displacement damage is due to α-decay and is therefore accumulated when the glasses have cooled down, hence after long storage time. Up to 10^{25} displacements/m^3 are reached, corresponding to a dpa level (displacements per atom) of up to and above 1, hence each atom of the glass is displaced at least once.

To achieve such high damage levels in an acceptable time, two techniques are used:

- doping with short-lived actinides (e.g. Pu-238, Cm-242, and Cm-244 with half-lives of 87.7, 0.4 and 18.1 years, respectively) replacing long-lived Np, Pu, and Am in the glass. In the following, results on R7T7 and GP 98/12 doped with 0.5 or 1.5 wt.% Cm-244 are reported;
- controlled ion implantation with heavy ions in the 10^2 keV energy range to simulate the recoil atoms of the α-decay. This technique is convenient and fast, the specimens can be easily handled since they are not radioactive, but a comparatively thin surface layer of ~ 20 to 100 nm depth only is damaged and, since external charged particles are used, an electric field may affect the results (see Section 3.4 and below).

The time-scales and damage levels of these three damage sources are very different. Typical values (depending on age and concentration of the waste, or on amount and type of short-lived actinides, or on ion current and ion dose) are

	time scale yrs	range of dpa achieved	range of dose rates, dpa/h
real waste matrix	10^5-10^6	up to 5	~ 5×10^{-9}
actinide doping	0.1 - 5	~ 5 achieved so far	~ 10^{-4}
ion implantation	10^{-4} - 10^{-6}	10^{-2} to 10^{-2}	~10^{-1} to 10^{2}

Considerations were therefore given to quantify possible dose rate effects; such effects would be expected in glasses because of the low recovery temperatures (~ 200 to 500 °C) of the damage and were in fact observed in measurements of Na-diffusion (see Section 3.4). The problem of largely varying dose rates was discussed at the workshop on radiation damage effects in nuclear waste materials [7] with the conclusion that damage recovery occurs both in real waste glasses as well as in laboratory work with actinide-doped glasses, but not in ion implanted glasses with the very high dose-rates.

The results on the Cm-244 doped glasses which accumulated damage levels simulating a storage time of ~ 100000 years can be summarized as follows:

Density and volume: small changes in density ($\Delta\rho$ in %) occurred up to a damage level of ~ 5×10^{24} α-decays m^{-3} which could be fitted to an ingrowth equation of the type

$$\Delta\rho = A(1-\exp\{-BD\})$$

where A is the change in density at saturation, B is the fraction of the glass totally damaged by each α-decay, and D is the dose (here in α-decays g^{-1}). For R7T7, the values are A = 0.55 ± 0.05 %, B = (0.095 ± 0.005)x10^{-17} g. Similar small densitiy changes (range ± 0.5 %) were found for other waste glasses [19]. The approach of a saturation value at ~ 5x10^{24} α-decays m^{-3} (~ 2x10^{18} αg^{-1}) suggests that an equilibrium state is reached between defect formation and instantaneous defect recovery at this damage level.

Leaching: Figs 7 and 8 show typical results for leaching of R7T7 and GP 98/12 glasses doped with Cm-244 as a function of damage up to a level corresponding to storage times of ~ 10^5 years. No significant effect of damage is seen, the leach rates tend rather to decrease than to increase. The total normalized mass loss (initial rate in the terms of Section 4) is plotted in Fig. 7. The conclusions of the above-mentioned workshop [7] contained, beyond else, the recommendation to perform solution analysis in addition to just reporting weight loss measurements which were regarded as "a poor indicator of actual glass dissolution". Therefore, both types of measurements were performed with R7T7, GP 98/12 (and the US glass MCC 76-68). Some 30 elements were analyzed, 4 of which are shown in Fig. 8. Not shown are the results of the other elements (including Na). The trend was always that of the total weight loss. We can thus conclude that the leaching behavior shows no significant variation due to radiation damage, if a realistic damage production (i.e. actinide doping) is used.

Mechanical properties: With the same glasses, hardness and fracture behavior were measured as a function of damage level, using indentation techniques [16, 17, 19]. The hardness decreased by ~ 30 % and both the probability of crack formation and the crack lengths formed at Vickers indentations decreased with increasing damage level (see Fig. 9), corresponding to very significant increases in fracture toughness K_{Ic} by up to 100 %. This behavior is explained to be most probably due to quenched-in stresses along the path of the recoil atoms of the α-decay and possibly be supported by He-bubble formation. The net result of the two above phenomena is reduced brittleness and better crack propagation resistance, hence a technologically positive effect.

Recent experiments [41, 42] with a Japanese borosilicate glass with a very high α-decay damage level (3x10^{25} α-decays/m^3, due to decay of Pu-238 or Cm-244) confirm the above results and show a decrease in the elastic modules, E, by about 30 %. All changes in H, K_{Ic} and E occurred within the first 2-3x10^{24} α-decays/m^3, as with the R7T7 and GP98 12 glasses. Annealing of the Japanese glasses led to

almost complete recovery of H and E at 400 °C, 10 h whereas K_{I_c} recovered only partly even at 450 °C, 48h. This result is *apparently* in contrast to that obtained on ion implanted R7T7 and GP 98/12 glasses (see below). Note, however, that the behavior of He formed by α-decay in the different Cm-doped glasses was apparently different as well: The Japanese glasses showed rather large He-bubbles (0.15 to 0.35 μm) at the highest damage level (without annealing), actually accounting for all of the observed density decrease, and these bubble shrank upon annealing. In contrast, the Cm-doped glass GP 98/12 with the highest damage level "foamed" to about twice the volume upon fast annealing to 500 °C, attributed to He precipitation [32]. There is no explanation at present for this different behavior.

Ion-implanted glasses: Very many studies have been performed with ion implanted glasses ever since the first report of largely increased aqueous corrosion due to high ion doses was reported from Orsay in 1980 [43]. Much of this work was devoted to the glasses R7T7 and GP 98 12 [e.g. 6, 7, 15, 16, 26, 44, 45]. The attractive aspects of ion implantation are the speed and ease to obtain high damage levels, the relative ease to vary the specimen temperature *during* damage production, simply by using a heating stage during implantation, and the ease to handle the damaged specimens. The drawbacks have been described above: a relatively thin surface layer only is damaged, foreign atoms are introduced, external charged beams are used setting up an electric field and causing incongruent sputtering of the surface and leading to biased Na-mobility thus potentially changing the properties of the glass.

The enhanced leaching in glasses implanted to doses $\geq 10^{14}$ ions/cm^2 reported first in ref. [43] was subsequently often confirmed, e.g. in the very recent experiment of Fig. 4 (full dots) with high dose Kr implants. It was also found in GP 98/12 and R7T7 glasses ion implanted at 350 °C. It was accompanied by enhanced hydration and surface enrichment in elements of low solubility (Ti, rare earths etc.). However, as with enhanced Na-diffusion (see Section 3.4), these chemical effects of ion implantation damage are due to high dose rates, surface sputtering and radiation enhanced Na mobility biased by the electric field set-up during implantation, hence to conditions imposed by ion implantation. They are thus not expected to occur in real waste glasses and they are not found in the glasses doped with short-lived actinides.

The technologically positive aspects of damage, i.e. the increased fracture toughness, K_{Ic}, was also found in ion implanted specimens [e.g. 44, 45]. This damage effect was largely absent if damage was formed above 250 °C. The tensile

stresses formed during implantation causing an increase in K_{Ic} recover thus at rather low temperatures.

Comparison with ceramic waste forms: A variety of ceramic waste forms was suggested as waste matrices (see Section 1 and ref. [1]) and some of them were extensively tested. Only a very brief summary on their behavior under α-decay can be given here. All of the ceramics tested in this respect (e.g. SYNROC, zirconolite, perovskite, $Ca_2Nd_8(SiO_4)_6O_2$ and others) swell; volume increases of up to 9 % were observed at saturation [19], quite in contrast to the very small volume changes in waste glasses. Also, at or slightly below the dose level causing saturation in swelling, a loss of crystallinity is observed, i.e. these ceramics become amorphous (metamict) [6, 7, 19, 46]. The radiation induced swelling and metamictization result in higher leach rates and increased fracture toughness, but decreased hardness. As an example, α-decay damaged zirconolite $CaZrTi_2O_7$ doped with short-lived Cm-244 showed an increase in leach rate of about a factor of 10 compared to crystalline, undamaged material, the fracture toughness went through a maximum ($K_{Ic} \sim 3\ MN/m^{3/2}$ compared to $\sim 1.7\ MN/m^{3/2}$), and the hardness decreased from 7.2 for undamaged zirconolite to 5.3 GPa for the metamict state [47]. In contrast to glasses, significant damage effects exist thus in these ceramics, especially for leaching.

A particular ceramic waste form is the spent fuel itself. Direct disposal of spent UO_2 fuel is presently investigated by many nations. High burnup UO_2 fuel is significantly different from the starting UO_2. Many important properties change during burnup, and the fuel is not a homogeneous matrix. Some of the fission products are released into the gap between fuel and clad, some precipitate at grain boundaries, the leach rate is indicated to increase significantly at high damage level [48] and at high burnup, the so-called rim effect [49] causes a grain subdivision process in the outermost 100 - 200 μm of the fuel, hence a structure enriched in actinides and fission products with a submicrometer grain size.

All these phenomena should be considered when comparing different waste forms.

6. Evaluation of the long-term behavior

From the results reported above, it is obvious that the initial corrosion rate decreases significantly under purely static conditions or when the solution renewal rate is low. Various experiments with R7T7 waste glass [50] have shown that if a residual corrosion rate exists, it is $< 2 \times 10^{-4}\ gm\ m^{-2} d^{-1}$, hence a factor of 10^4

lower than the initial corrosion rate. At such a rate, more than 10^{n} years would be necessary to alter the glass block. The conclusion is thus, that the corrosion kinetics under saturation conditions are not a problem for the long-term storage.

Rather, the important parameters will be the solution renewal rate and any other phenomenon which can decrease the H_2SiO_4 activity below the saturation level of a^*_{Si}. Two main processes may act in this sense: precipitation of silicated materials, and consumption of Si by environmental materials in the near field. The importance of these two processes can be estimated as follows:

New phases: crystallized phases are known to form on the gel layers of waste glasses during long exposure to aqueous solutions, mainly by a dissolution-reprecipitation process. Many surface studies have been performed to identify these crystalline phases. At 90 °C (and with the R7T7 glass) practically no such phases were found. Therefore, hydrothermal alteration experiments were extended up to 250 °C. The major alteration products formed at high temperatures are clays (smectite), aluminosilicates (zeolites) and hydrated calcium silicates. Sophisticated complex geochemical modelling is necessary to decide whether - and under which conditions - these minerals are liable to control the long-term Si activity in solution. The geochemical modelling activity for R7T7 [51] shows that the minerals identified to be formed at the glass surface tend to delay the onset of saturation but do not control the long-term Si activity in the solution. One does therefore not expect a renewal of glass corrosion due to their formation.

Environmental near-field materials: experiments with GP 98/12, R7T7 and other glasses with a number of environmental materials (see e.g. ref. [52] for R7T7) have shown that container materials as well as clay, granite or salt can have a secondary effect on the kinetics of glass alteration. For instance, most clays act as silica sinks, consuming Si released from the glass, thus delaying or preventing the increase in Si concentration to saturation conditions. The result is corrosion of the glass at a higher rate than that in the presence of other materials.

7. Conclusions

Tailor-made nuclear waste glasses, carefully selected to allow incorporation of some 30 different oxides occurring in high level waste, HLW, solutions, as the French product R7T7, exhibit a very small degree of recrystallization, and their physical and chemical properties are very similar to those of high quality industrial glasses, and e.g. superior to those of conventional "window glass".

The nuclear waste glasses have been shown to withstand α-decay doses corresponding to $> 10^5$ years under repository conditions without significant modifications of their properties.

A difficult problem is predicting the long-term behavior of HLW glasses subjected to aqueous corrosion in the presence of different near-field materials. Since there are no straightforward means of simulating glass alteration in a deep underground geological formation over geological time spans, mathematical models are needed for predictions of glass alteration. A substantial research effort was devoted to identifying the basic corrosion mechanisms liable to control the long-term alteration. These mechanisms are now rather well understood: the basis for developing geochemical models is thus existing. Realistic conditions are known to exist under which glass alteration rates are very low. The glass can thus fulfill its role as first containment barrier of several tens of thousands of years for todays HLW solutions. In combination with additional engineered barriers and considering the very long-term retention capacity of the geological repository itself, underground disposal of vitrified nuclear waste can be suggested to be an appropriately safe solution for future generations.

References

[1] W. Lutze and R. C. Ewing, Radioactive Waste Forms for the Future, North Holland (1988)

[2] F. Pacaud, C. Fillet, G. Baudin and H. Bastien-Thiry, 2nd Int. Seminar on Radioactive Waste Products, Julich, May (1990) p. 577

[3] L. Kahl, M.C. Ruiz-Lopez, J. Saidl and Th. Dippel, Kernforschungszentrum Karlsruhe, Report KfK-3251 (1982), in German

[4] B. Kienzler, Mat. Res. Soc. Proc. Vol. 127 (1989) 191

[5] W.J. Weber and F.P. Roberts, Nucl. Technol. 60 (1983) 178

[6] Hj. Matzke, Nuclear Waste Materials, Chapter 12 in Ion Beam Modification of Insulators, Eds. P. Mazzoldi and G.W. Arnold, Elsevier (1987) p. 501

[7] Hj. Matzke, Nuclear Waste Materials, Special issue for a workshop on Radiation Damage Effects in Nuclear Waste Materials, Nucl. Instrum. Methods in Phys. Research B 32 (1988) 453-517

[8] E. Vernaz and J.L. Dussossoy, Appl. Geochem., Suppl. Issue 1 (1992) 13

[9] F. Delage, D. Ghaleb, J.L. Dussossoy, O. Chevallier and E. Vernaz, J. Nucl. Mater. 190 (1992) 1991

[10] G.W. Arnold, G. DellaMea, J.C. Dran, H. Kawahara, P. Lehuede, Hj. Matzke, P. Mazzoldi, M. Noshiro and C. Pantano, Glass Technology 31 (1990) 58

[11] H. Bach, P. Großkopf, P. March and F. Rauch, Glastech. Ber. 60 (1987) 21 and 33

[12] Chemical Durability and Related Properties of Solidified High-Level Waste Forms, IAEA Technical Report Series No. 257, Vienna (1985)

[13] V.L. Stolyarova, presented during 8 STNM, this conference (1992)

[14] E. Vernaz, P. Deymier and N. Jacquet-Francillon, in Nuclear Waste Management I, eds. G.G. Wicks and W.A. Ross, Advances in Ceramics, Vol. 8 (1984) 687

[15] Hj. Matzke, ed., Indentation Fracture and Mechanical Properties of Ceramic Fuels and of Waste Ceramics and Glasses, Special volume Europ. Appl. Res. Reports, Harwood Acad. Publ., London 7, Nr. 7 (1987)

[16] Hj. Matzke and E. Toscano, eds., Indentation Techniques, special volume Europ. Appl. Res. Reports, Harwood Acad. Publ., London (1990)

[17] Hj. Matzke and E. Toscano, ibid., p. 1403

[18] R. Dal Maschio, Hj. Matzke and G. DellaMea, ibid., p. 1389

[19] E. Vernaz, A. Loida, G. Malow, J.A.C. Marples and Hj. Matzke, in Long Term Stability of Radioactive Waste Forms, Proc. 3rd EC Conf. on Radioactive Waste Management and Disposal, Luxembourg, Sept. 1990, Ed. L. Cecille, Elsevier (1991) p. 302

[20] A.M. Bevilacqua and Hj. Matzke, in ref. [16], p. 1369

[21] R. Dal Maschio, E. Toscano and Hj. Matzke, in ref. [15], p. 1001

[22] Hj. Matzke, E. Toscano, J.L. Routbort and K. Reimann, J. Amer. Ceram. Soc. 69 (1986) C-138

[23] F. Dyment, Hj. Matzke and E. Toscano, J. Non-Cryst. Solids 93 (1987) 22

[24] Hj. Matzke, in Thermodynamics of Nuclear Materials 1979, IAEA (Vienna) I (1980) 311

[25] M. Thomas and Hj. Matzke, J. Amer. Ceram. Soc. 72 (1989) 146

[26] Hj. Matzke, E. Toscano and G. Linker, Nucl. Instrum. Meth. in Physics Research B 32 (1988) 508

[27] M. Yamashita, Hj. Matzke and G. Linker, Mat. Res. Soc. Symp. Proc. 257 (1992) 183

[28] M. Yamashita and Hj. Matzke, in Modifications Induced by Irradiation in Glasses, Ed. P. Mazzoldi, Elsevier (1992) p. 53

[29] P. Mazzoldi and A. Miotello, Rad. Effects 98 (1986) 39

[30] A. Miotello and F. Toigo, Nucl. Instrum. Meth. in Physics Research B 32 (1988) 258

[31] G. DellaMea, C. Rossi-Alvarez, G. Mazzi, G. Bezzon, J. Chaumont, J.C. Dran, M. Mendenhall and J.C. Petit, Nucl. Instrum. Meth. in Physics Research B 19/20 (1987) 943

[32] Hj. Matzke, unpublished results (1992)

[33] L. Kahl, PhD Thesis, D 83, University of Berlin (1974)

[34] Hj. Matzke, J. Nucl. Mater. 114 (1983) 121

[35] International standard ISO 6962-1982 (E) (1982)

[36] F. Delage and J.L. Dussossoy, Mat. Res. Soc. Symp. Proc. 212 (1991) 41

[37] T. Advocat, J.L. Crovisier and E. Vernaz, Mat. Res. Soc. Symp. Proc. 212 (1991) 57

[38] B. Grambow, Mat. Res. Soc. Symp. Proc. 44 (1985) 15

[39] E. Mouche and E. Vernaz, Mat. Res. Soc. Symp. Proc. 112 (1988) 703

[40] W.G. Burns, A.E. Hughes, J.A.C. Marples, R.S. Nelson and A.M. Stoneham, J. Nucl. Mater. 107 (1982) 245

[41] Y. Inagaki, H. Furuya, K. Idemitsu, T. Banba, S. Matsumoto and S. Muraoka, Mat. Res. Soc. Symp. Proc. 257 (1992) 199

[42] Y. Inagaki, H. Furuya, Y. Ono, K. Idemitsu, T. Banba, S. Matsumoto and S. Muraoka, Mat. Res. Soc. Symp. Proc. XVI Symp. Scientific Basis of Waste Management, Boston, Nov. (1992)

[43] J.C. Dran, M. Maurette and J. C. Petit, Science 209 (1980) 1518

[44] Hj. Matzke, G. Della Mea, J.C. Dran, G. Linker and B. Tiveron, Nucl. Instrum. Meth. in Physics Research B 46 (1990) 256

[45] Hj. Matzke, G. Della Mea, J.C. Dran, V. Rigato and A. Bevilacqua, in Modifications Induced by Irradiation in Glasses, Ed. P. Mazzoldi, Elsevier (1992) p. 25

[46] W.J. Weber and Hj. Matzke, Radiation Effects 98 (1986) 93

[47] W.J. Weber, J.W. Wald and Hj. Matzke, J. Nucl. Mater. 138 (1986) 196

[48] Hj. Matzke, J. Nucl. Mater. 190 (1992) 101

[49] Hj. Matzke, J. Nucl. Mater. 189 (1992) 141

[50] E. Vernaz, T. Advocat and J.L. Dussossoy, Nucl. Waste Management, ed. G.B. Mellinger, Cer. Trans. (Am. Cer. Soc.) 9 (1989) 175

[51] T. Advocat, J.L. Crovisier, B. Fritz and E. Vernaz, Mat. Res. Soc. Symp. Proc. 176 (1990) 291

[52] N. Godon, E. Vernaz, J.H. Thomassin and J.C. Touray, Mat. Res. Soc. Symp. Proc. 127 (1989) 97

[53] F. Delage, PhD-Thesis, Univ. Montpellier, France (1992)

Figure Captions

Fig. 1 Arrhenius diagram for diffusion of elements occurring in the HLW in the waste glass GP 98 12 (or VG 98 12), and U-diffusion in a precursor glass [23-28, 33]

Fig. 2 Typical time dependence of U-diffusion into a borosilicate glass (precursor of GP 98/12) showing the effect of recrystallization at 570 °C.

Fig. 3 Normalized mass loss of the waste glass R7T7 in water in dynamic and static leaching experiments

Fig. 4 Tracer experiments with R7T7 glass implanted with 40 keV Kr-85 ions to measure the slow kinetics of leaching at room temperature

Fig. 5 Schematic model of the main mechanisms of aqueous corrosion of waste glasses

Fig. 6 Modelling of glass dissolution: evolution with time of measured and calculated concentrations of Si and B for a dynamic experiment (90 °C, H_2O, 122 ml/d) [52]

Fig. 7 Leach rate (14d, 150 °C, H_2O static test) as a function of α-decay damage for the glasses R7T7 and GP 98/12 doped with Cm-244

Fig. 8 Content in solution of Si, B, Ca and Mo for the glass R7T7 of Fig. 7

Fig. 9 Dependence of hardness, H, crack length, c, at Vickers indentations and probability to form these cracks in the waste glass R7T7 as a function of α-decay damage

Table 1: Composition (wt.%) of the two waste glasses R7T7 and GP 98/12

Composition in wt.%

	R7T7	GP 98/12		R7T7	GP 98/12
SiO_2	45.48	48.32	AgO_2	0.03	-
Al_2O_3	4.91	2.25	CdO	0.03	-
B_2O_3	14.02	10.68	SnO_2	0.02	0.02
Na_2O	9.86	14.89	Sb_2O_3	0.01	-
CaO	4.04	3.45	TeO_2	0.23	0.25
MgO	-	1.84	BaO	0.60	0.71
ZnO	2.50	-	La_2O_3	0.56	0.58
TiO_2	-	3.97	Ce_2O_3	0.93	1.18
LiO_2	1.98	-	Pr_2O_3	0.44	0.56
Fe_2O_3	2.91	0.28	Sm_2O_3	0.31	0.39
P_2O_5	0.28	-	Gd_2O_3	0.03	0.06
ZrO_2	2.65	1.95	Nd_2O_3	1.59	1.87
NiO	0.42	0.11	Rb_2O	0.13	0.17
Cr_2O_3	0.51	-	Cs_2O	1.29	1.00
SrO	0.33	0.38	RuO_2	0.46	0.84
Y_2O_3	0.20	0.23	Rh_2O_3	0.12	0.15
MoO_3	1.70	2.02	PdO	0.33	0.55
MnO_2	0.25	0.51	ThO_2	0.33*	-
			UO_2	0.52	0.80*

*(simulating the total content of NpO_2, PuO_2, AmO_2, CmO_2 in the glass)

Table 2: The two waste glasses R7T7 and GP 98/12

Property	Glass	
	R7T7	GP 98/12
density, g/cm^3	2.75	2.83
mean thermal expansion coefficient, K^{-1} (25-300 °C)	8.3 x 10^{-6}	8.1 x 10^{-6}
thermal conductivity at 20 °C, WK^{-1}m^{-1}	1.1	1.1
viscosity at 1100 °C, Pa·s	8	21
transformation temperature, °C	502	543
Young's modulus, E, GPa	84	81.7
fracture toughness, K_{Ic}, MPam$^{1/2}$	0.95	0.86

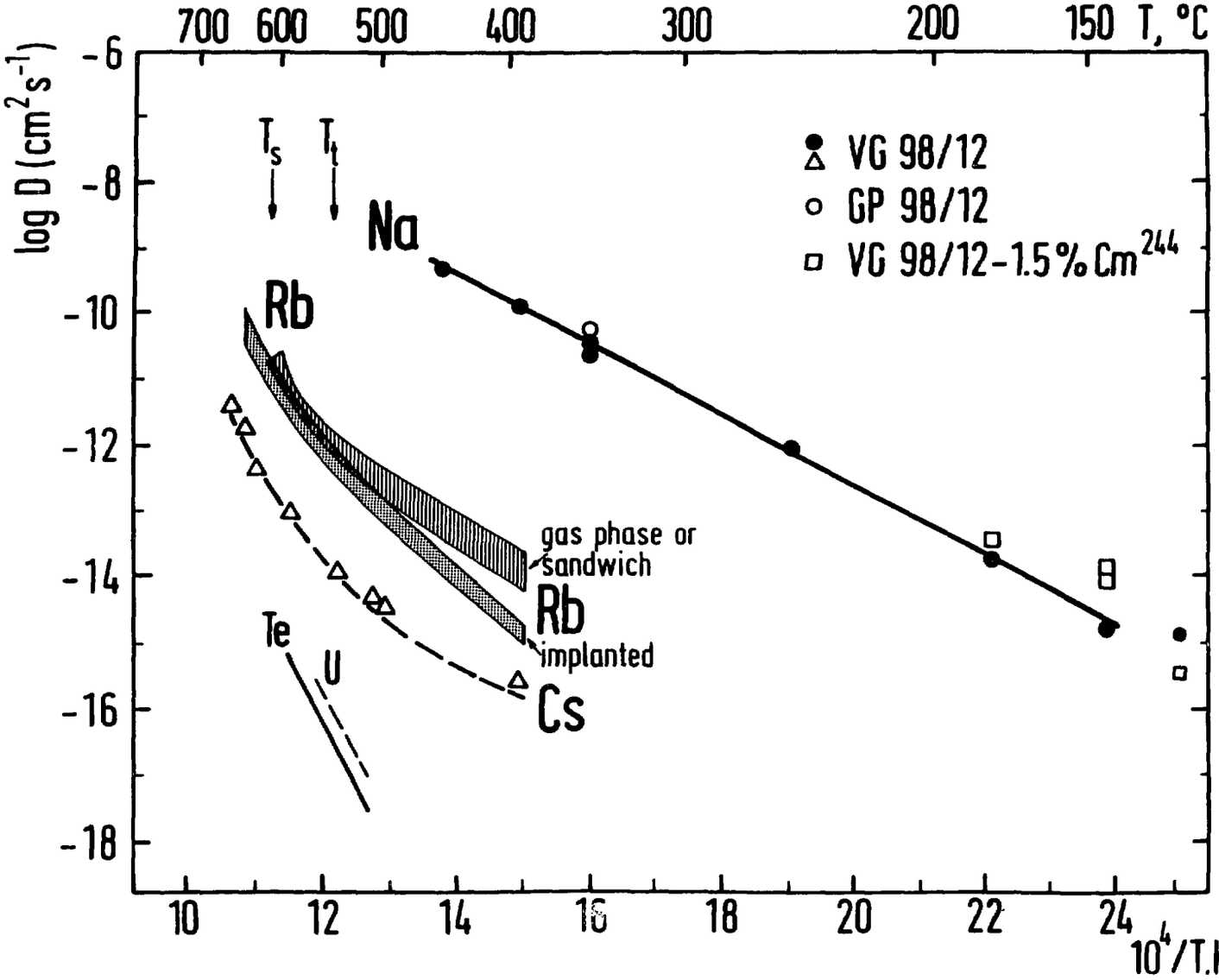
700 600 500 400 300 200 150 T, °C
log D (cm²s⁻¹)
-6
-8
-10
-12
-14
-16
-18
T_s
T_t
Na
Rb
gas phase or sandwich
Rb implanted
Cs
Te
U
VG 98/12
GP 98/12
VG 98/12-1.5% Cm²⁴⁴
10 12 14 16 18 20 22 24
10⁴/T.K⁻¹

Fig. 1

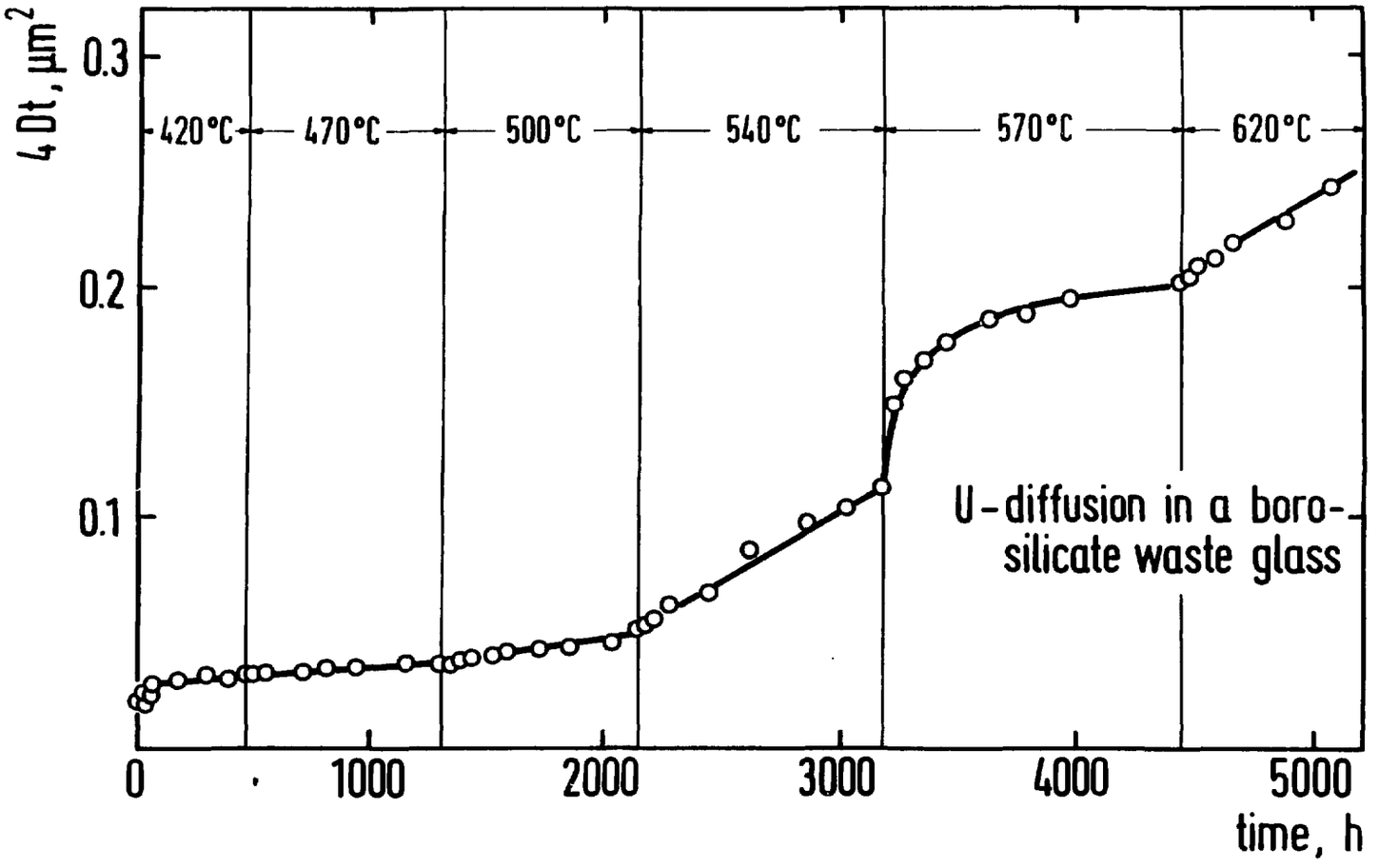
4 Dt, µm²
0.3
0.2
0.1
420°C
470°C
500°C
540°C
570°C
620°C
U-diffusion in a boro-silicate waste glass
0
1000
2000
3000
4000
5000
time, h

Fig 2

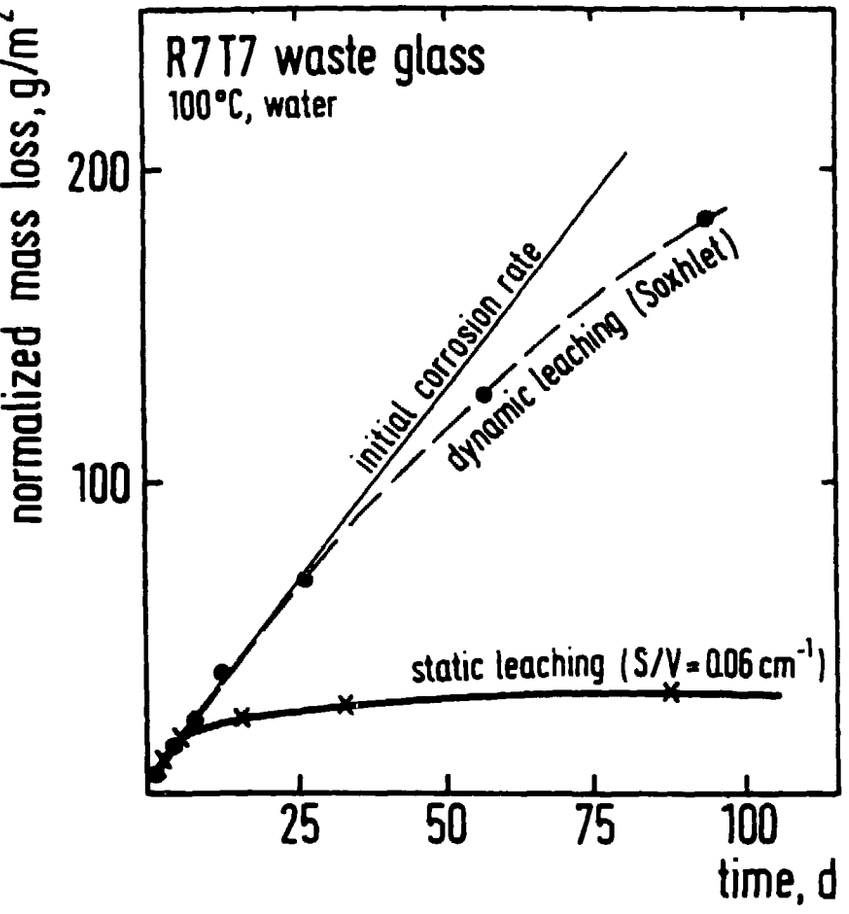
R7T7 waste glass
100°C, water
normalized mass loss, g/m²
200
100
initial corrosion rate
dynamic leaching (Soxhlet)
static leaching (S/V = 0.06 cm⁻¹)
25
50
75
100
time, d

Fig 3

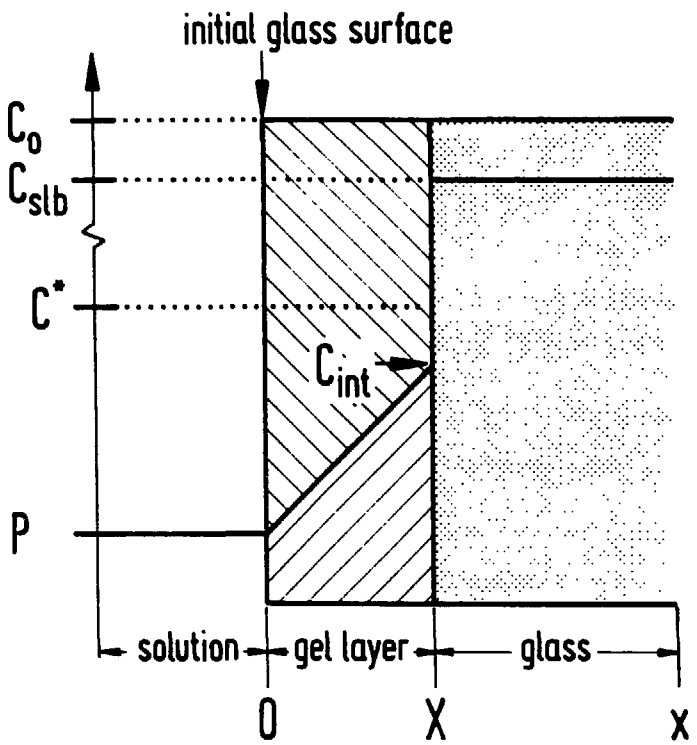
initial glass surface
C_o
C_{slb}
C^*
C_{int}
P
solution
gel layer
glass
0
X
x

Fig 5

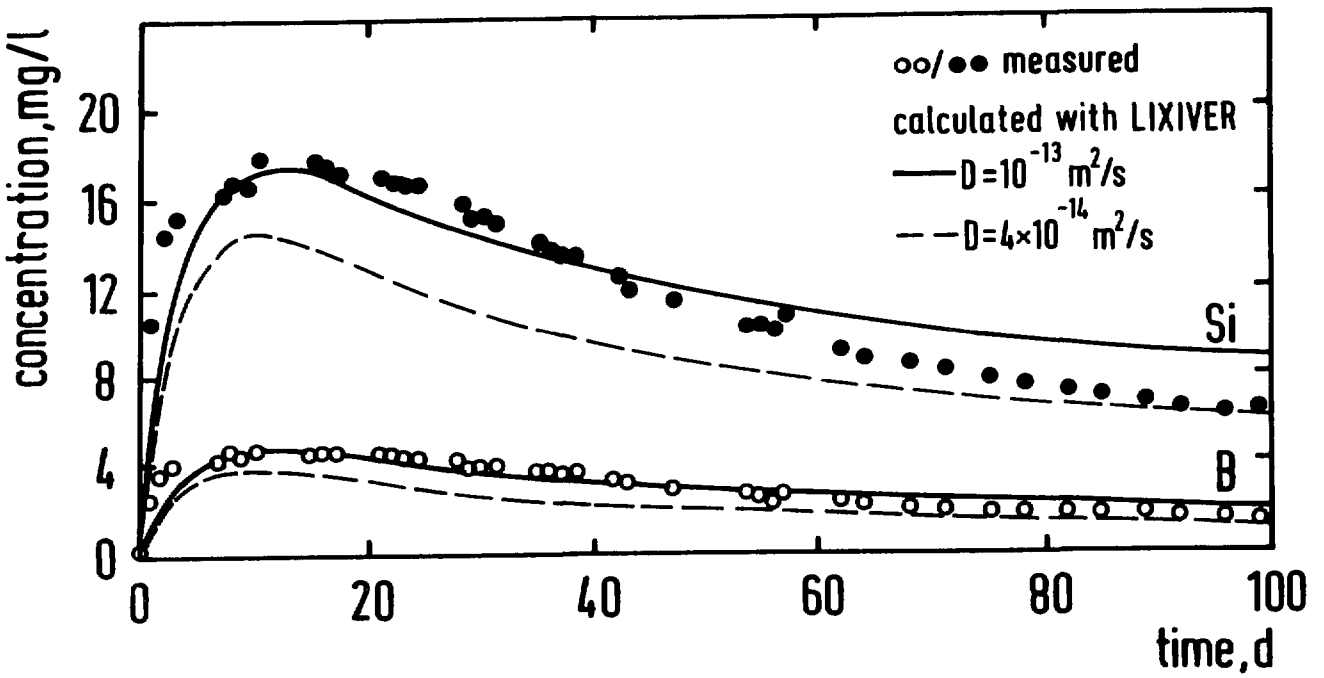
concentration, mg/l
20
16
12
8
4
0
0
20
40
60
80
100
time, d
oo/●● measured
calculated with LIXIVER
——D=10⁻¹³ m²/s
– – D=4×10⁻¹⁴ m²/s
Si
B

Fig 6

Fig. 7

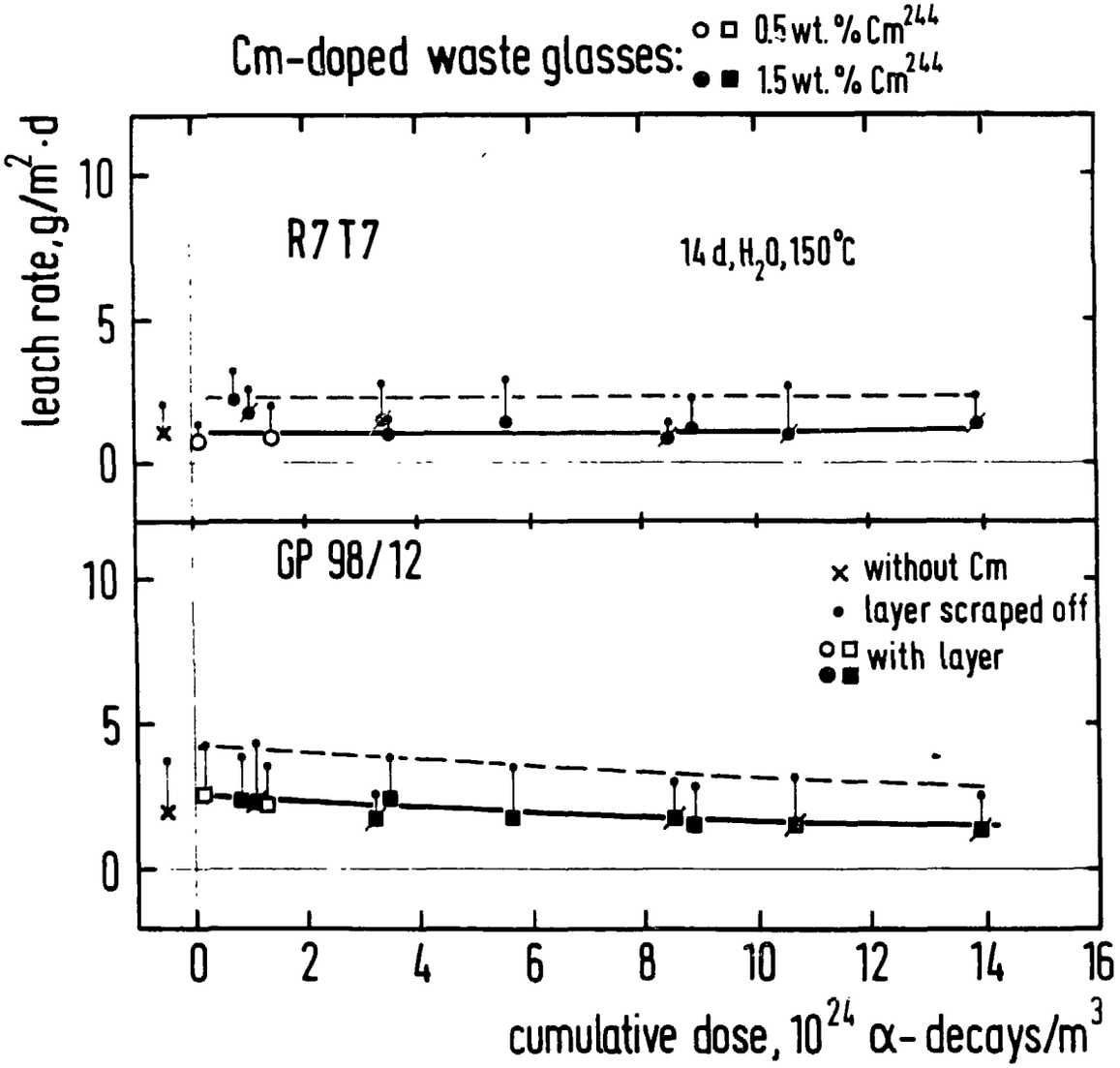
Cm-doped waste glasses:
0.5 wt. % Cm244
1.5 wt. % Cm244
leach rate, g/m2·d
R7 T7
14 d, H2O, 150°C
GP 98/12
without Cm
layer scraped off
with layer
cumulative dose, 10^24 α-decays/m3

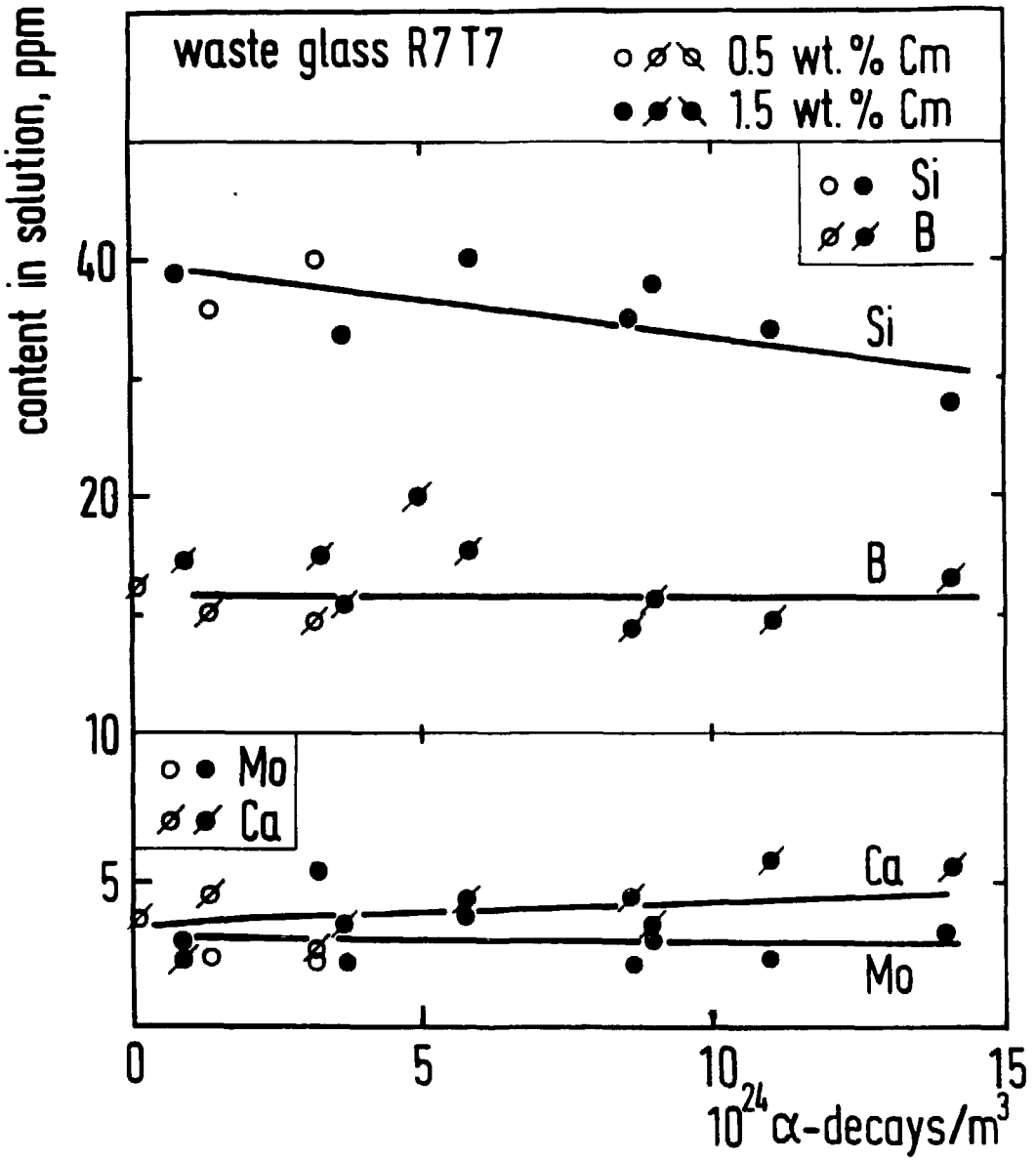
waste glass R7 T7
0.5 wt.% Cm
1.5 wt.% Cm
Si
B
Mo
Ca
content in solution, ppm
40
20
10
5
0
5
10
15
10^{24} α-decays/m^3

Fig 8

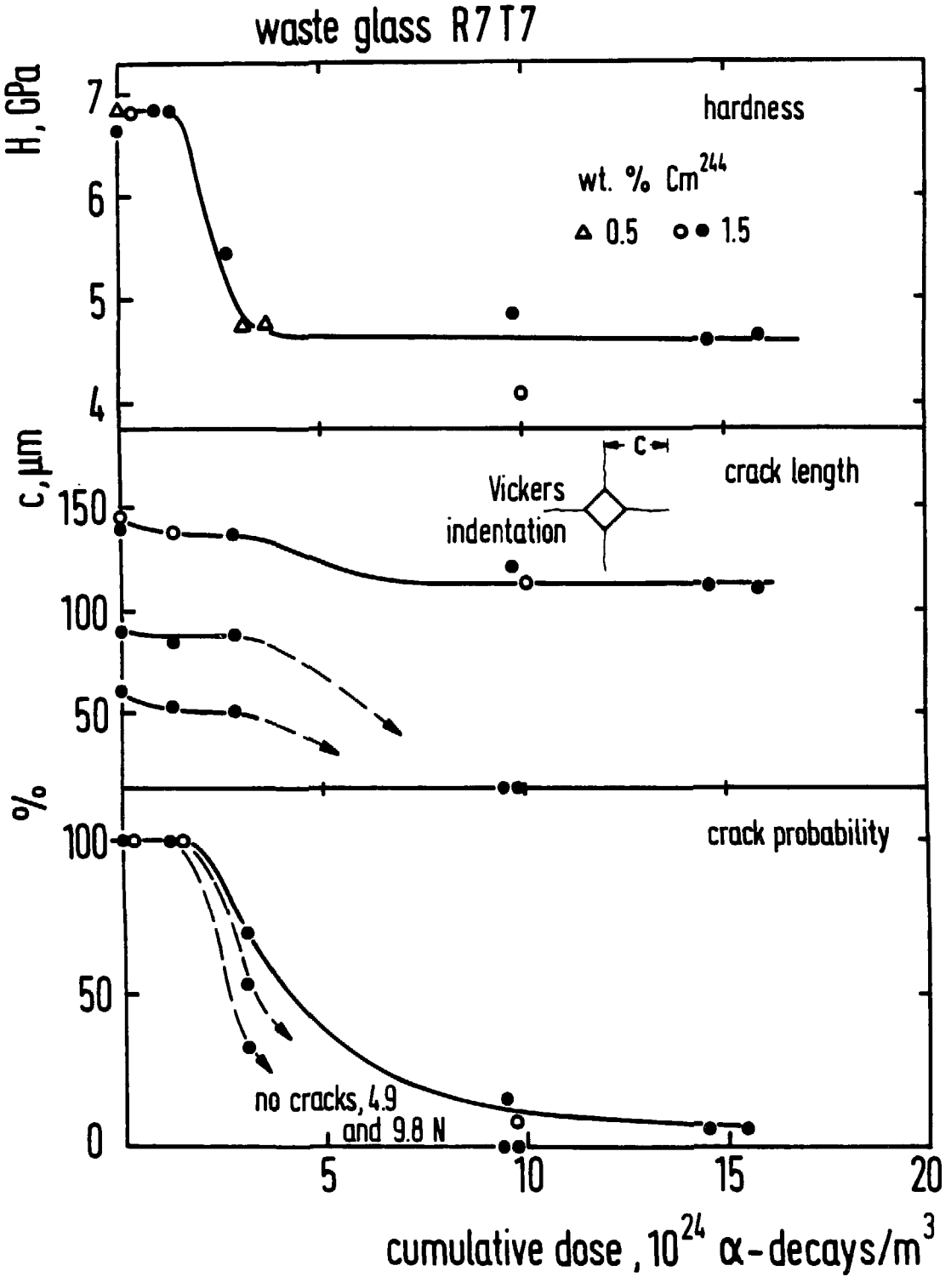
waste glass R7T7
H, GPa
hardness
wt. % Cm244
0.5
1.5
c, µm
crack length
Vickers
indentation
%
crack probability
no cracks, 4.9
and 9.8 N
cumulative dose, 10^24 α-decays/m^3

Fig 9